

Continuous X-ray diffraction measurement of lattice rotation during tensile deformation of aluminium crystals

NARAYAN R. JOSHI,* ROBERT E. GREEN, Jr

Mechanics and Materials Science Department, The Johns Hopkins University, Baltimore, Maryland 21218, USA

Results are reported of experimental measurements in which crystallographic orientation changes due to lattice rotation were continuously monitored during uniaxial tensile tests on 99.99% pure aluminium crystals. The use of an image intensifier tube, lens coupled to a fluorescent screen, permitted Laue transmission X-ray diffraction patterns to be recorded with a motion picture camera at rates as fast as 24 frames per second. In all tests, the lattice rotation caused the tensile axes to overshoot the $[100]-[111]$ symmetry line contrary to the classical view. In general, the experimentally measured lattice rotation values lagged behind the theoretical values as derived from the idealized single slip model. No clear dependence of lattice rotation on strain rate was found, although in every test the lattice rotated fast initially with no bending evident and then the lattice rotation slowed down accompanied by considerable lattice bending.

1. Introduction

The classical formulae of Taylor and Elam [1, 2] and Göler and Sachs [3] offer an oversimplified idealized picture of the mechanism of lattice rotation during the plastic deformation of metal single crystals subjected to uniaxial tensile stress. An extensive survey of face-centred-cubic single-crystal deformation data has markedly demonstrated the general invalidity of these classical formulae [4]. In reality, many factors not considered in the classical treatment cause the crystal to deform in a complex manner which yields the experimentally observed lattice rotation. Ahlers and Haasen [5] found that small but systematic deviations from single-crystal glide occur during the deformation of silver single crystals which could be explained by secondary slip in addition to slip on the most highly stressed primary system. Mitchell and Thorton [6] tried to estimate the amount of secondary slip in Cu and α -brass single crystals deformed in uniaxial tensile tests. They used the standard Laue back-reflection technique

to estimate local deviations of successive orientations from those obtained through theoretical calculations assuming single slip on the primary system. Johnson [7] used the same Laue back-reflection technique to estimate the amount of secondary slip in copper single crystals through study of orientation changes. Tisone *et al.* [8] studied the overshoot phenomenon (i.e. overshoot of the orientation of the crystal tensile axis across the stereographic $[100]-[111]$ symmetry line) in Cu-15 at.% Al single crystals as a function of quenching temperature, testing temperature and initial tensile axis orientation. They used the X-ray back-reflection technique to determine orientations periodically during tensile testing of the specimens. Overshooting was found by them to be independent of orientation and test temperature, but the degree of overshoot appeared to increase with increasing quench temperature. Their results also showed that the overshoot was not a direct function of the stacking fault energy in the range of 5 to 10 erg cm⁻² for a Cu-15 at.% Al

* Present address: Associate Professor, Coppin State College, Baltimore, Maryland 21216, USA.

alloy. Piercy *et al.* [9] investigated the cause of overshoot of the crystal orientation across the symmetry line during tensile deformation of alpha-brass single crystals. They measured the orientations of specimens *in situ* during the tensile experiments by means of the back-reflection Laue method. Their tensile experiments were performed on a hard machine with a normal strain rate of $4.2 \times 10^{-5} \text{ sec}^{-1}$. The orientation measurements were made initially at 0.2% primary extension and finally at 4% extension on the conjugate system. They found that the amounts of easy glide and overshoot did not vary appreciably as a function of initial orientation. Their data confirmed also the old hypothesis of latent hardening of the conjugate slip system. They concluded that overshooting in alpha-brass crystals is due to latent hardening of the conjugate slip system rather than softening processes in the active primary slip system. In all these and many other prior measurements of lattice rotations, the tensile test was stopped in order to make a Laue X-ray diffraction photograph from which the crystallographic orientation was determined. Often the test crystals were removed from the testing machine in order to X-ray them. Haasen and Kelly [10] found a small yield-point effect during interrupted tensile tests on single crystals of pure aluminium and nickel. According to them, the effect is a result of the arrangement of dislocations during unloading rather than a thermally activated migration of point defects to dislocations. The present authors, therefore, felt a need to measure continuously lattice rotations in uninterrupted tests on single crystals to avoid complexities such as the yield-point effect, relaxation and recovery. It should also be noted here that in addition to interrupted testing, factors such as elongation rate, test temperature, size effects and grip constraints limit uniform homogeneous rotation of the lattice.

Since prior experimental methods have not permitted a study of continuous measurements of lattice rotation during tensile tests, the present work was undertaken in order to make such a study. In 1968, Reifsnider and Green [11, 12] developed an electro-optical system which incorporates a cascaded image intensifier tube and permits direct viewing and recording of Laue transmission X-ray diffraction patterns during tensile deformation of single-crystals. In the present work this electro-optical system was used to study quantitatively continuous orientation

changes due to lattice rotation of aluminium single crystals deformed with different strain rates in uninterrupted uniaxial tensile tests.

2. Experimental procedure

A schematic diagram of the experimental arrangement is shown in Fig. 1. A Machlett AEG-50-S tungsten target X-ray tube, operated at 50 kV and 40 mA, served as the X-ray source. A pin-hole collimator served to reduce the diameter of the incident X-ray beam to 0.1 mm prior to impingement on the centre of the test specimen. The test crystals were grown from 99.99% pure aluminium using the gang mould modified Bridgman method of Chen and Pond [13]. This method yielded 24 specimens of common orientation from one heat. Each of these specimens was of $0.3175 \text{ cm} \times 0.3175 \text{ cm}$ cross-section, had a gauge length of 7.62 cm, and had enlarged 0.635 cm by 0.635 cm by 0.3175 cm button heads at both ends which fitted matching slots in the tensile machine grips. The as-grown crystals were carefully clipped from the gate, etched in aqua regia, and annealed at 600°C for 24 h and furnace-cooled. After preparing many groups of single-crystal specimens, one crystal from each group was X-rayed using the Laue transmission X-ray diffraction technique with a Polaroid XR-7 Land Diffraction Cassette and its initial orientation was determined. Two groups of crystals were chosen for the experimental measurements, the initial orientations of which are shown in the standard stereographic triangle of Fig. 2. As can be seen, the test specimens from group 3 possessed initial axial orientations in the central portion of the standard triangle but close enough to the $[100]$ – $[111]$ symmetry line that lattice rotation during tensile deformation brought the axial orientation to this line prior to fracture. The initial glide elements of specimens from group 3 were $\lambda_0 = 39^\circ$ and $\phi_0 = 54^\circ$, where λ_0 is the angle between the tensile axis and the slip direction and ϕ_0 is the angle between the tensile axis and the normal to the slip plane. The specimens from group 6 possessed initial axial orientations very close to the $[100]$ – $[111]$ symmetry line such that very little lattice rotation was required during tensile deformation to bring the axial orientation to this line. The initial glide elements of specimens from group 6 were $\lambda_0 = 32^\circ$ and $\phi_0 = 62^\circ$.

The tensile tests were performed at room temperature on a table model Instron tensile test

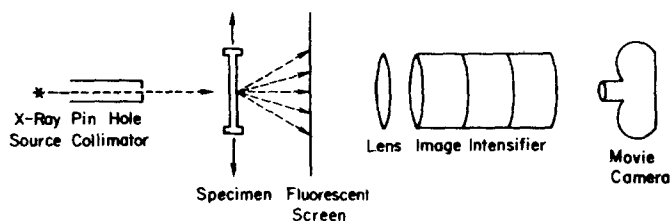


Figure 1 Schematic drawing of experimental apparatus.

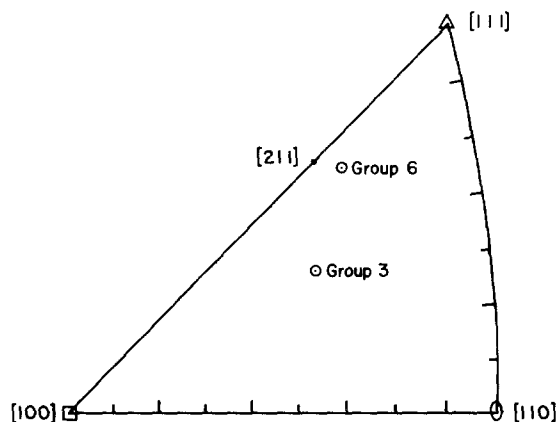


Figure 2 Initial orientations of tensile axes of specimens.

machine. The test specimen was held by gimballed grips with slots into which the button heads fitted. In this manner it was not necessary to apply any force whatsoever to the single crystal specimen prior to the start of elongation. Table I shows the nomenclature used to label each test, along with the recording camera speed, and the elongation rate of the tensile test machine. The first entry 3F(10) signifies a specimen from group 3 tested at a fast rate of 10 cm min^{-1} . The last entry 6S(0.01) signifies a specimen from group 6 tested at a slow rate of 0.01 cm min^{-1} .

On one side of the specimen mounted on the Instron testing machine, the X-ray tube was positioned. On the other side, at a distance of 3 cm from it, a 6 in. diameter DuPont CB-2 fluorescent

screen was positioned to transform the Laue transmission X-ray diffraction image into a visible one. A Super Farron $f/0.87$, 72 mm coupling lens, corrected for 4 to 1 demagnification, transmitted the visible image to the image tube. The image intensifier used was a three-stage magnetically focused RCA type C70021A with an S-20 input photocathode and a P-20 output phosphor. The image tube was of unity magnification with useful input and output screen diameters of 40 mm.

The image on the output phosphor was recorded using a 16mm Bolex Model HL movie camera fitted with a Canon $f/0.95$, 50 mm lens. Framing rates of 24 and 12 frames sec^{-1} were obtained using a motor drive. The slower time lapse framing rates were obtained using a Samenco Movie Control Unit, Model MC-5E50, and a solenoid activated shutter release. All recording was done on Kodak Linagraph Shellburst film.

The initial orientation of each crystal specimen tested was determined from the first frame of the movie recorded during the tensile test. All initial orientations thus determined coincided with those determined previously by the conventional Laue transmission X-ray diffraction technique using the Polaroid Cassette. The accuracy in determining the initial orientations of undeformed crystal specimens was approximately 1° , while orientation determinations at the latter stages of the tensile tests were limited to an accuracy of about 3° because of the pronounced asterism in the Laue spots due to bending of the lattice planes associated

TABLE I Test details

Specimen and test	Camera speed (frames sec^{-1})	Speed of cross-head (cm min^{-1})	Average strain rate (sec^{-1})
3F(10)	24	10	2.2×10^{-4}
3F(5)	12	5	1.1×10^{-4}
3S(0.05)	1 frame/60 sec	0.05	1.1×10^{-6}
3S(0.01)	1 frame/12 sec	0.01	2.2×10^{-7}
6F(10)	24	10	2.2×10^{-4}
6F(5)	12	5	1.1×10^{-4}
6S(0.05)	1 frame/60 sec	0.05	1.1×10^{-6}
6S(0.01)	1 frame/12 sec	0.01	2.2×10^{-7}

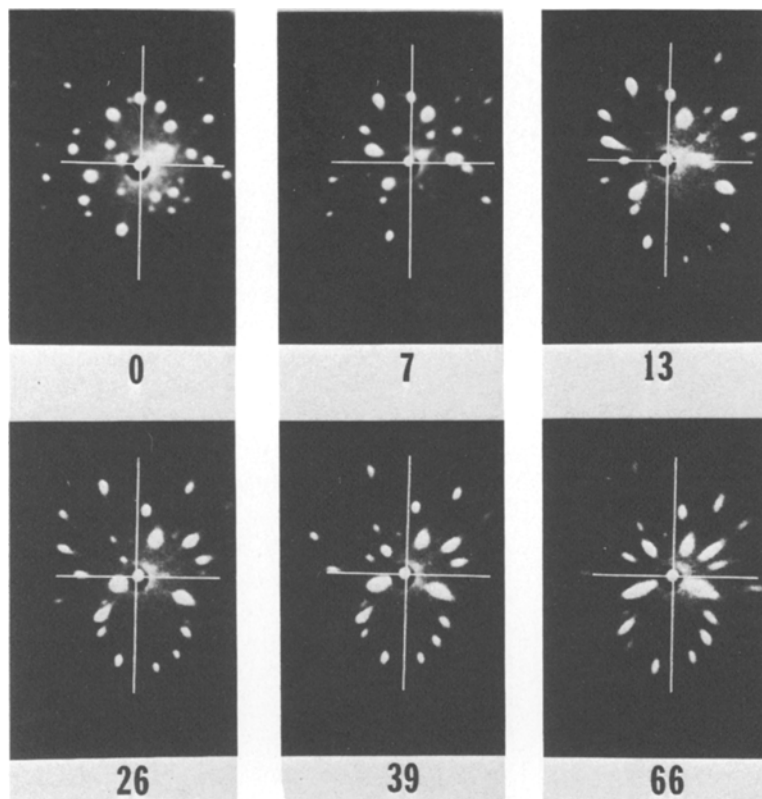


Figure 3 Laue X-ray transmission motion picture frames at various stages of tensile strain as labelled.

with the interplay between substantial plastic deformation and the constraints of the specimen grips.

Fig. 3 shows a series of Laue transmission X-ray diffraction patterns as recorded on the motion picture film at six different strain values for an aluminium single crystal subjected to uniaxial tensile elongation along an axis parallel to the length of the figure. The centre of the white cross superimposed on each photograph indicates the location of the direct X-ray beam, while the long vertical arm of each cross indicates the direction of the tensile axis. It should be noted that the specimen is initially oriented for single slip on the primary slip system and that at about 13% strain the specimen crystal lattice has rotated so that both primary and conjugate slip systems are favoured geometrically (two ellipses of Laue spots approximately the same size), but due to latent hardening on the conjugate slip system the specimen continues to rotate past the symmetry line until fracture finally occurs at 66% strain. As will be shown in later figures, the amount of lattice rotation is large at first (up to about 13% strain in

this case) and then decreases in the latter stages of elongation even though the tensile test machine cross-head continues to move at a constant rate. The general tendency is for rapid lattice rotation to occur without significant bending of the lattice planes and then for decreased lattice rotation to occur and more bending of the planes to prevail. The increased asterism in the latter frames as compared with the first several frames due to this augmented lattice bending is clearly evident.

3. Experimental results and discussion

Figs. 4 and 5 show the experimental results obtained using specimens from group 3 tested at the fast and slow rates, respectively. Figs. 6 and 7 show similar results obtained using specimens from group 6. Although the movie film record permits experimental determination of a continuous curve to represent the lattice rotation, each tensile axis position shown in Figs. 4 to 7 was obtained by analysing every 25th frame of the motion picture record to avoid overcrowding of points on these diagrams. The numbers by the side of some points indicate the corresponding strain values. All

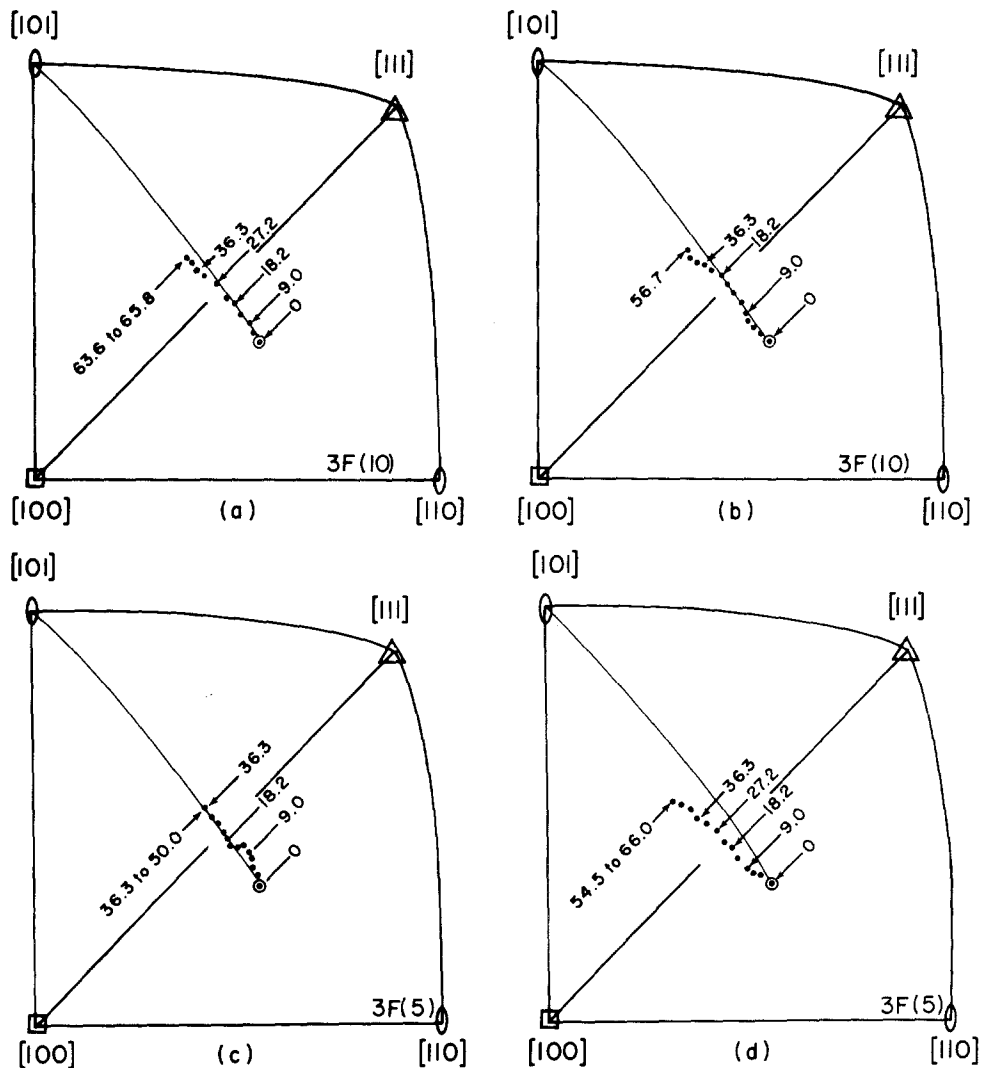


Figure 4 Lattice rotations for crystals from group 3 tested at fast rates: (a) and (b) 10 cm min^{-1} , (c) and (d) 5 cm min^{-1} . The arrows indicate % strain.

specimens were pulled in tension until fracture occurred.

In all tests the tensile axes overshot the $[100]$ – $[111]$ symmetry line irrespective of either the rate of strain or the initial orientation. The great circle, drawn as a solid line in Figs. 4 to 7, connects the initial orientation to the $[101]$ pole and shows the path of the specimen axis in the ideal single slip lattice rotation situation. Overshooting of the tensile axes in all tests confirms the preponderance of primary slip beyond the symmetry line. In most of the experiments conducted, the path of the tensile axis deviated from the solid line path, associated with single slip behaviour, after crossing the symmetry line and in

some cases deviations occurred before the tensile axis crossed the symmetry line. These results are similar to those obtained earlier by other investigators and can be explained by considering the time of initiation of secondary slip relative to intersection of the tensile axis with the symmetry line. If secondary slip occurs earlier than predicted classically, i.e. prior to arrival of the tensile axis at the symmetry line, deviations from the single slip path will be observed. If secondary slip is delayed because of latent hardening, deviations from the single slip path will not be observed, even though the tensile axis has crossed the symmetry line where secondary slip should be initiated according to the classical viewpoint.

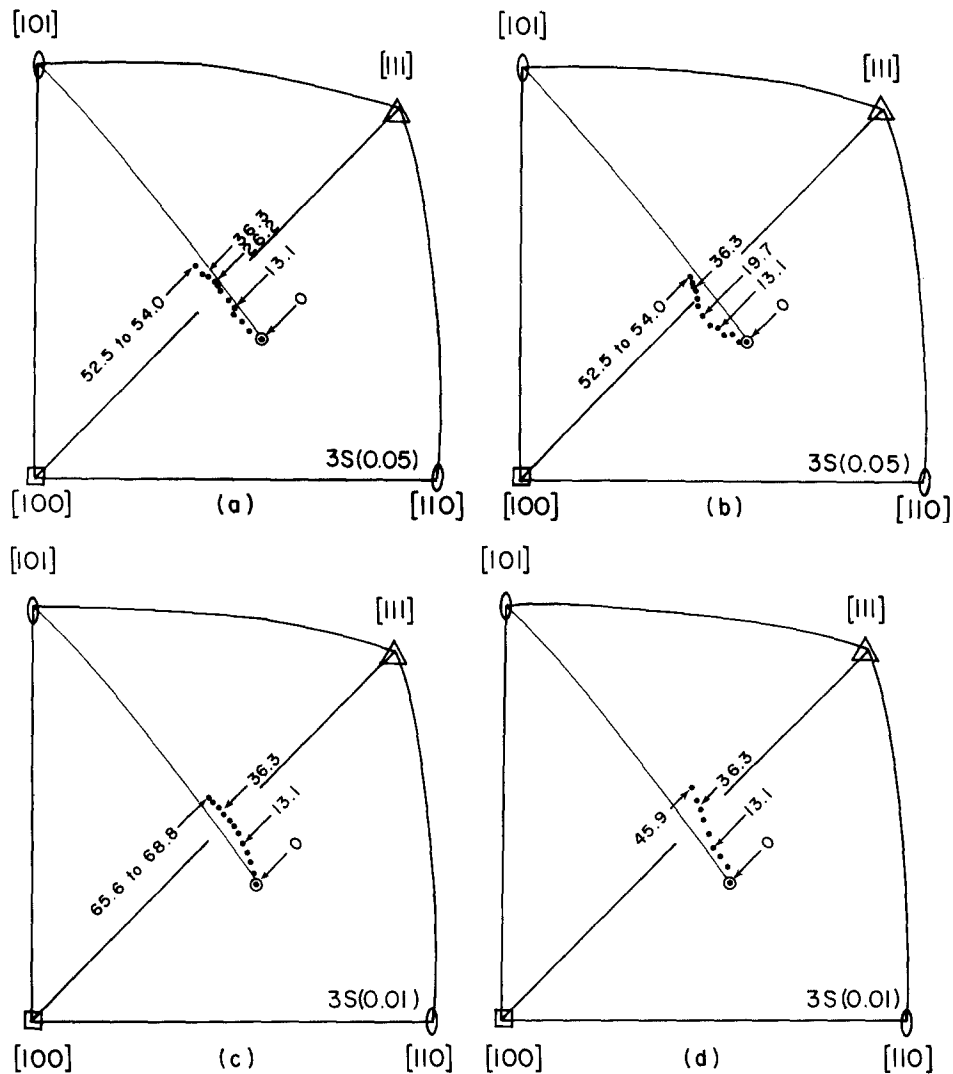


Figure 5 Lattice rotations for crystals from group 3 tested at slow rates: (a) and (b) 0.05 cm min^{-1} , (c) and (d) 0.01 cm min^{-1} . The arrows indicate % strain.

A careful observation of these continuously monitored paths of the tensile axes shows some interesting features not reported previously in the literature. The experimentally determined lattice rotation paths of the tensile axes show a tendency to deviate to the left of the solid line single slip path for fast tests and to the right of the solid line single slip path for slow tests. The deviation to the left of the great circle solid line single slip path means moving away from the $[211]$ direction, the final destination of the tensile axis in classical double slip theory. The deviation to the right of the great circle means moving towards the $[211]$ direction. The results in Figs. 4 to 7 indicate that the observed lattice rotation is much

more influenced by secondary slip in slow tests than in fast tests.

The lattice rotation of a number of test specimens slowed down at or beyond approximately 35% strain even though fracture did not occur until larger strain values. In order to make a comparative evaluation between the different tests, the orientation of the specimen axis was indicated at the 36.3% strain level in each of the stereographic triangles in Figs. 4 to 7. Also indicated in Figs. 4 to 7 are the strain levels at which the specimen axes ceased to rotate and fracture occurred. As can be seen in most cases, even though the specimen axes stopped rotating, the specimen still required more strain in order to fracture.

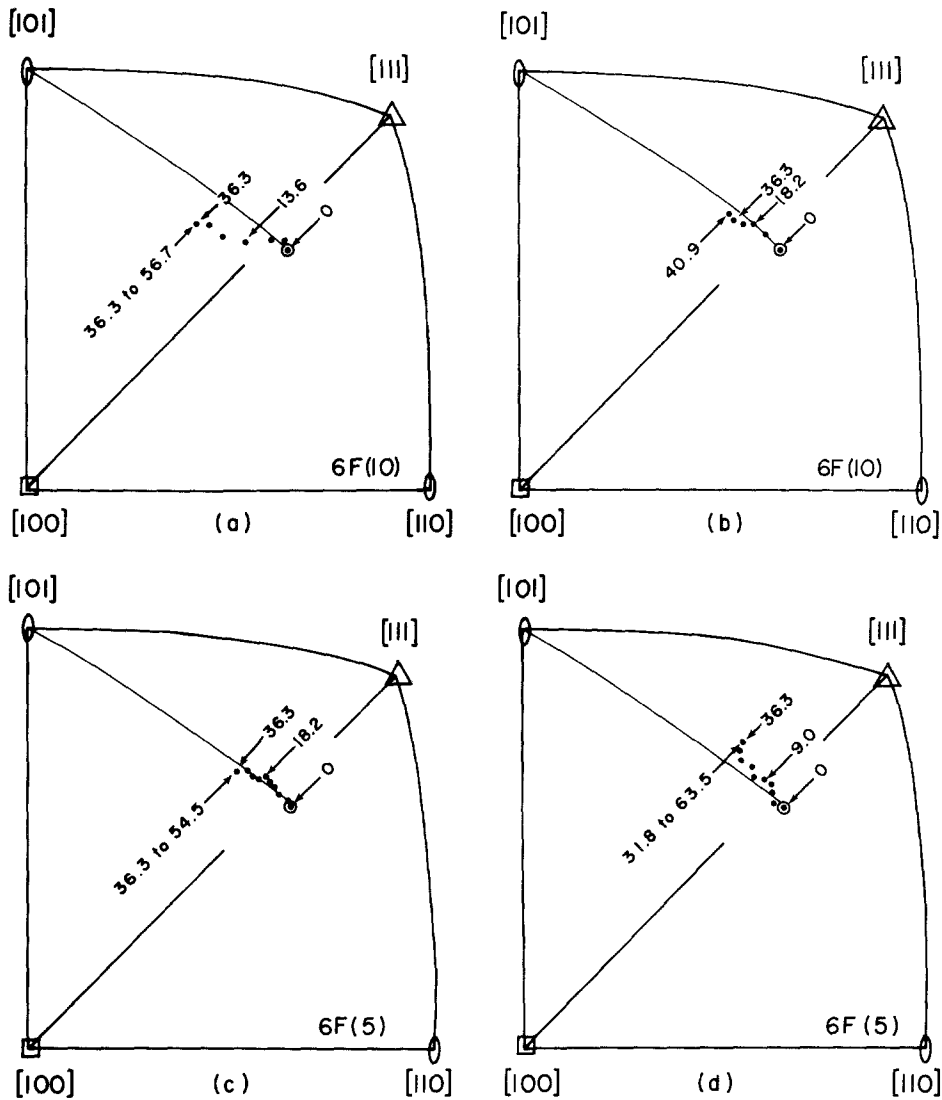


Figure 6 Lattice rotations for crystals from group 6 tested at fast rates: (a) and (b) 10 cm min^{-1} , (c) and (d) 5 cm min^{-1} . The arrows indicate % strain.

Figs. 8 and 9 show plots of angle of lattice rotation θ versus % strain ϵ for specimens of group 3. Figs. 10 and 11 show similar plots for specimens of group 6. For convenience of comparison, the theoretical single slip lattice rotation versus % strain curve is also added to each of these plots. This theoretical curve is shown by a continuous solid line. The theoretical values of lattice rotation for various strain values were obtained from the relation [14]

$$\theta = \lambda_0 - \sin^{-1} \left(\frac{l_0}{l} \sin \lambda_0 \right), \quad (1)$$

where l_0 is the initial length and l is the instantaneous length both parallel to the tensile axis.

Of the four curves of fast tests on specimens from group 3 (Fig. 8), two lie above the theoretical curve and two lie below the theoretical curve. Of the four curves of slow tests on specimens from group 3 (Fig. 9), all four lie below the theoretical curve. It appears, therefore, that lattice rotation angles in slow tests show greater tendency to lag the theoretical values than those in fast tests. At a given strain level, on the average for the specimens of group 3, fast tests show slightly higher lattice rotation values than slow tests at a given

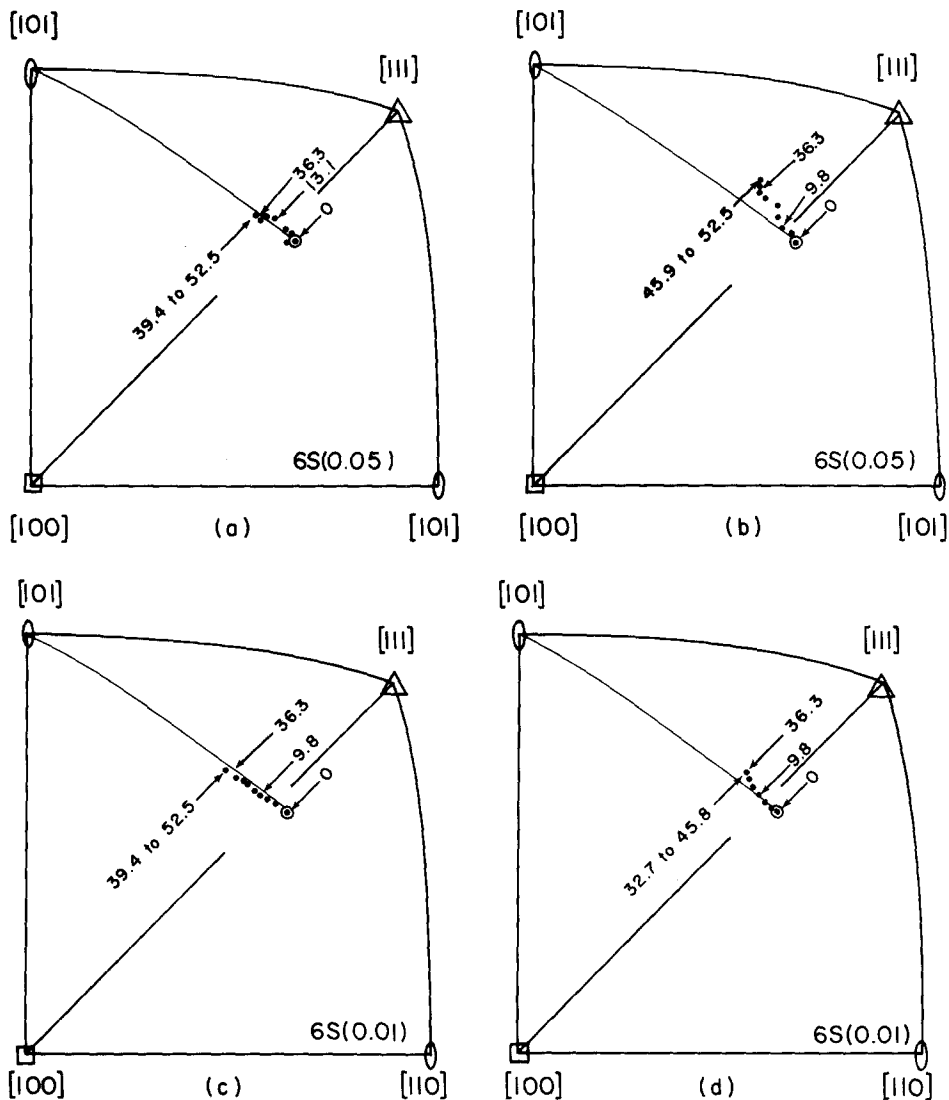


Figure 7 Lattice rotations for crystals from group 6 tested at slow rates: (a) and (b) 0.05 cm min^{-1} , (c) and (d) 0.01 cm min^{-1} . The arrows indicate % strain.

strain level. No such difference in values of lattice rotation is found among slow and fast tests on specimens from group 6. However, lattice rotation values in tests on specimens from group 6 do lag considerably behind the corresponding theoretical values.

4. Conclusions

In all uniaxial tensile tests performed on 99.99% purity aluminium single crystals, the tensile axes overshoot the $[100]-[111]$ symmetry line.

Specimens with initial axial orientations away from the symmetry line and well inside the stan-

dard stereographic triangle favour more rotation of the tensile axes than specimens with initial orientations near the symmetry line when the specimen is extended to the same strain level.

In almost all tests, experimentally observed lattice rotation values lag behind the theoretical ones derived from the single slip formula corresponding to the same strain levels.

No clear dependence of lattice rotation on strain rate is found although the fast tests on specimens from group 3 showed slightly higher lattice rotation than the slow tests on specimens from the same group.

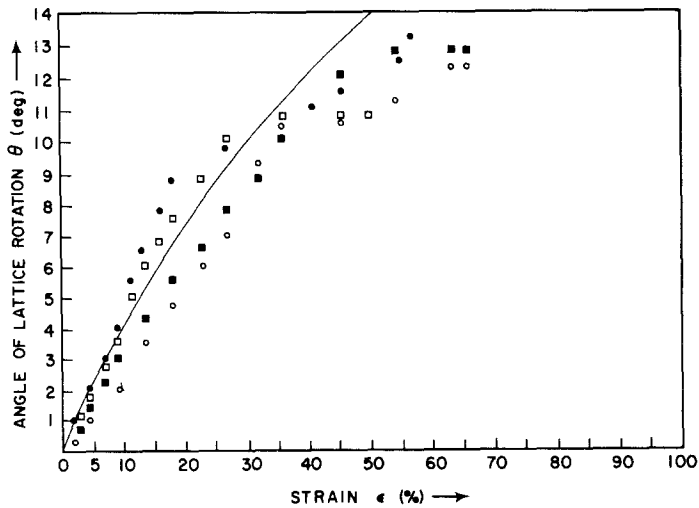


Figure 8 Angles of lattice rotation versus strain for specimens of group 3: \circ, \bullet 10 cm min^{-1} cross-head speed; \square, \blacksquare 5 cm min^{-1} cross-head speed. The continuous curve is the theoretical plot of lattice rotation assuming idealized single slip.

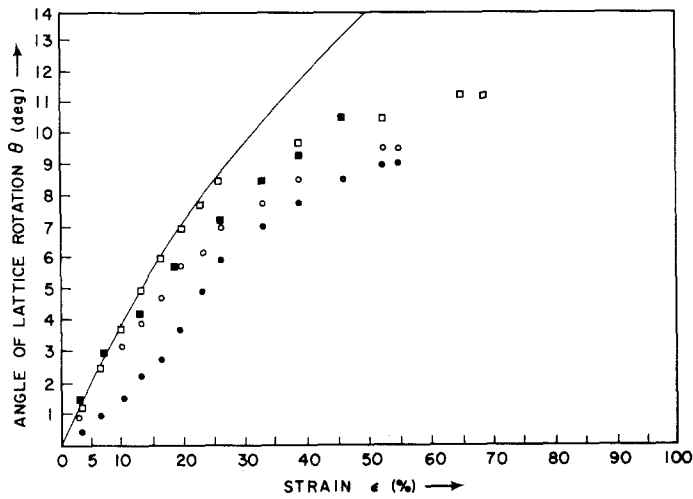


Figure 9 Angle of lattice rotation versus strain for specimens of group 3: \circ, \bullet 0.05 cm min^{-1} cross-head speed; \square, \blacksquare 0.01 cm min^{-1} cross-head speed. The continuous curve is the theoretical plot of lattice rotation assuming idealized single slip.

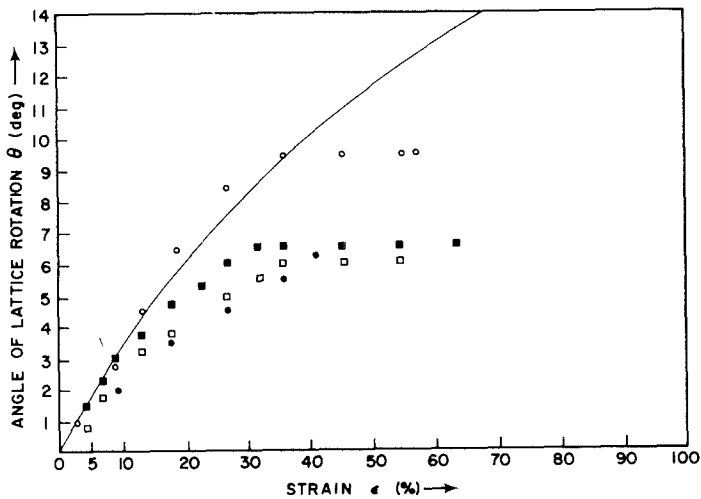


Figure 10 Angle of lattice rotation versus strain for specimens of group 6: \circ, \bullet 10 cm min^{-1} cross-head speed; \square, \blacksquare 5 cm min^{-1} cross-head speed. The continuous curve is the theoretical plot of lattice rotation assuming idealized single slip.

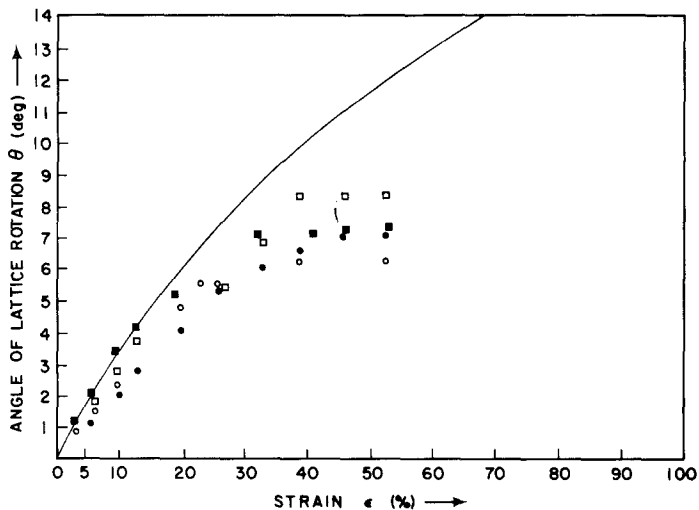


Figure 11 Angle of lattice rotation versus strain for specimens of group 6: ○, ● 0.05 cm min⁻¹ cross-head speed; □, ■ 0.01 cm min⁻¹ cross-head speed. The continuous curve is the theoretical plot of lattice rotation assuming idealized single slip.

The experimental measurement of the amount of lattice rotation and of subsequent overshooting offers information about the latent hardening of the secondary slip system produced by straining of single crystals oriented initially for single slip. The anisotropy of the flow stress may be closely related to the anisotropy of the dislocation distribution produced by single slip. In aluminium single crystals it was observed that the dependence of the anisotropy of the flow stress on the strain rate was low. Thus in all sixteen tests described in this work, the tensile axes overshoot the symmetry line, the observed lattice rotations lagged the theoretically calculated rotations, but not much dependence of lattice rotations on the strain rate was observed.

References

1. G. I. TAYLOR and C. F. ELAM, *Proc. Roy. Soc.* **102** (1923) 643.
2. *Idem, ibid.* **108** (1925) 28.
3. F. VON GÖLER and G. SACHS, *Z. Phys.* **41** (1927) 103.
4. J. F. BELL and R. E. GREEN Jr, *Phil. Mag.* **15** (1967) 469.
5. M. AHLERS and P. HAASEN, *Acta Met.* **10** (1962) 977.
6. T. E. MITCHELL and P. R. THORNTON, *Phil. Mag.* **10** (1964) 315.
7. L. JOHNSON, *Trans. Met. Soc. AIME* **245** (1969) 275.
8. T. C. TISON, J. O. BRITAIN and M. MESHI, *Phys. Stat. Sol.* **36** (1969) 479.
9. G. R. PIERCY, R. W. CAHN and A. H. COTTRELL, *Acta Met.* **3** (1955) 331.
10. P. HAASEN and A. KELLY, *Acta Met.* **5** (1957) 192.
11. K. REIFSNIDER and R. E. GREEN, Jr, *Rev. Sci. Instrum.* **39** (1968) 1651.
12. *Idem, Trans. Met. Soc.* **245** (1969) 1615.
13. N. K. CHEN and R. B. POND, *J. Met.* **4** (1952) 1085.
14. E. SCHMID and W. BOAS, "Plasticity of Crystals", English Translation (Hughes, London, 1950).

Received 7 March and accepted 26 July 1979.